Estuarine, Coastal and Shelf Science 83 (2009) 392–402

Contents lists available at ScienceDirect

Estuarine, Coastal and Shelf Science

journal homepage: www.elsevier.com/locate/ecss

Benthic metabolism and the fate of dissolved inorganic nitrogen in intertidal sediments

W.P. Porubsky [a], N.B. Weston [b], S.B. Joye [a,*]

[a] Department of Marine Sciences, The University of Georgia, Athens, GA 30602, USA
[b] Department of Geography and the Environment, Villanova University, Villanova, PA 19085, USA

ARTICLE INFO

Article history:
Received 7 July 2008
Accepted 3 April 2009
Available online 18 April 2009

Keywords:
intertidal sediments
benthic microalgae
denitrification
dissimilatory nitrate reduction to ammonium
anammox

Regional index terms:
USA
Georgia
Satilla River
South Carolina
Okatee River

ABSTRACT

We determined patterns of benthic metabolism and examined the relative importance of denitrification (DNF) and dissimilatory nitrate reduction to ammonium (DNRA) as sinks for nitrate (NO_3^-) in intertidal sediments in the presence and absence of benthic microalgal (BMA) activity. By influencing the activity of BMA, light regulated the metabolic status of the sediments, and, in turn, exerted strong control on sediment nitrogen dynamics and the fate of inorganic nitrogen. A pulsed addition of ^{15}N-labeled NO_3^- tracked the effect and fate of dissolved inorganic nitrogen (DIN) in the system. Under illuminated conditions, BMA communities influenced benthic fluxes directly, via DIN uptake, and indirectly, by altering the oxygen penetration depth. Under dark hypoxic and anoxic conditions, the fate of water column NO_3^- was determined largely by three competing dissimilatory reductive processes; DNF, DNRA, and, on one occasion, anaerobic ammonium oxidation (anammox). Mass balance of the added ^{15}N tracer illustrated that DNF accounted for a maximum of 48.2% of the $^{15}NO_3^-$ reduced while DNRA (a minimum of 11.4%) and anammox (a minimum of 2.2%) accounted for much less. A slurry experiment was employed to further examine the partitioning between DNF and DNRA. High sulfide concentrations negatively impacted rates of both processes, while high DOC:NO_3^- ratios favored DNRA over DNF.

1. Introduction

Nutrient regeneration in sediments and subsequent release to the overlying water column, commonly referred to as benthic-pelagic coupling, fuels a significant portion of water column production in shallow estuarine systems (Nixon et al., 1976). Water depth, turbidity, sedimentation rates, organic matter remineralization rates, bioturbation, and diffusive or advective transport influence the magnitude and efficiency of benthic–pelagic coupling (Aller, 1994; Jahnke et al., 2000). The presence and activity of a benthic microalgal community also strongly affects benthic–pelagic coupling (Joye et al., 1996; Jahnke et al., 2000). Benthic microalgae (BMA) occupy a μm to mm thick layer at the surface of intertidal and shallow subtidal sediments, and their activity affects both the oxygen (O_2) flux and the O_2 penetration depth in the sediment. By modulating O_2 dynamics, BMA alter the sediment redox status and influence rates and pathways of nutrient cycling. BMA also consume nutrients from both the water column and underlying sediments. Under oxic conditions, BMA-dominated sediments act as a nutrient sink, while under hypoxic or anoxic conditions the same sediments serve as a nutrient source to the water column (Joye et al., 1996; Eyre and Ferguson, 2002).

Oxygen production by BMA can stimulate nitrification, which may enhance dissimilatory nitrate (NO_3^-) sinks (An and Joye, 2001), e.g., denitrification (DNF) or dissimilatory nitrate reduction to ammonium (DNRA). Complete DNF is the reduction of NO_3^- to N_2 as described by (Zumft, 1992; Eq. (1)):

$$2NO_3^- + 5H_2 + 2H^+ \rightarrow N_2 + 6H_2O \quad (1)$$

The reduction of NO_3^- to N_2 via DNF involves a $5e^-$ transfer and has a free energy yield of -560 kJ mole^{-1} NO_3^- (Zumft, 1992). DNF produces mainly gaseous end products (N_2O and N_2), which readily diffuse from a system and are not generally bioavailable (Howarth et al., 1988); thus, DNF represents a net loss of fixed nitrogen from a system. Conversely, the end product of DNRA is NH_4^+, which is readily assimilable and can support additional production. The DNRA reaction includes NO_3^- reduction to NO_2^- and then to NH_4^+ (Tiedje, 1994; Thauer et al., 1977; Eq. (2)):

* Corresponding author. Room 220 Marine Sciences Building, Athens, GA 30602-3636, USA.
E-mail address: mjoye@uga.edu (S.B. Joye).

0272-7714/$ – see front matter © 2009 Elsevier Ltd. All rights reserved.
doi:10.1016/j.ecss.2009.04.012

$$NO_3^- + 4H_2 + 2H^+ \rightarrow NH_4^+ + 3H_2O \quad (2)$$

DNRA involves $8e^-$ per NO_3^- reduced and has a free energy yield of -600 kJ mole^{-1} NO_3^- (Thauer et al., 1977). The interaction between DNF and DNRA is further complicated by recent evidence for a third pathway of NO_3^- reduction: anaerobic ammonium oxidation (anammox). Anammox involves the production of N_2 via the reduction of NO_2^- coupled to the oxidation of NH_4^+ (van de Graaf et al., 1995; Eq. (3)):

$$NO_2^- + NH_4^+ \rightarrow N_2 + 2H_2O \quad (3)$$

Anammox has a free energy yield of -358 kJ mole^{-1} NO_2^- (van de Graaf et al., 1995). Like DNF, anammox generates N_2 and thus represents a net loss of nitrogen from the system.

DNF, DNRA, and anammox may compete for nitrogen oxides (NO_3^- or NO_2^-) in sediments in the absence of O_2 and influence the DIN form available for flux to the overlying water column. The relative importance of DNRA versus DNF as NO_3^- sinks in coastal systems is unclear; however, DNRA rates rival DNF rates in some environments (Koike and Hattori, 1978; An and Gardner, 2002). While no previous studies have examined the interaction between these three processes, a number of studies have examined the relative importance of DNF versus DNRA. The environmental controls on these two processes include the ratio of dissolved organic carbon (DOC) to NO_3^- (Tiedje et al., 1982), temperature (Ogilvie et al., 1997), NO_3^- concentration (Fazzolari et al., 1998), and hydrogen sulfide (H_2S) concentration (Brunet and Garcia-Gil, 1996). The controls on anammox are uncertain, and how anammox interacts with DNF and DNRA is not known. Available evidence suggests that anammox and DNF can occur simultaneously (Thamdrup and Dalsgaard, 2002; Risgaard-Petersen et al., 2003), and anammox bacteria may be capable of DNRA (Kartal et al., 2007).

We used sediment flux core incubations and ^{15}N amendments to examine interactions between BMA activity and dissimilatory NO_3^- sinks in intertidal coastal sediments in Georgia and South Carolina, USA. We hypothesized that under diel, illuminated conditions, a pulse of DIN supplied to the water column would be assimilated by BMA. In contrast, under dark induced, anoxic conditions, DIN would be reduced by one of the three dissimilatory pathways. The relative importance of the dissimilatory processes has implications for the nitrogen budget of the system; thus, it is important to understand their regulation individually and collectively. Slurry experiments were used to investigate the impact of H_2S concentration and the DOC:NO_3^- ratio on the partitioning of dissimilatory NO_3^- reduction between DNF and DNRA. The results provide insight into the interactions between benthic photosynthesis, DNF, DNRA and anammox.

2. Methods

2.1. Study sites

Two tidal creek bank sites in Georgia and South Carolina, USA (Fig. 1) were sampled in January/February and August of 2002 and January of 2004 for benthic flux experiments, and in December 2005 for slurry experiments. At both sites, the adjacent saltmarsh was dominated by *Spartina alterniflora*. Creek bank sediments were macrophyte free but overlain by dense accumulations of benthic microalgae, mainly diatoms.

The Dover Bluff (DB) site, located on Umbrella Creek along the Satilla River (Georgia), has annual salinity and temperature ranges of approximately 12–30 and 15.5–25.6 °C, respectively. The site lies adjacent to a residential community and receives septic inputs from the developed upland (Weston et al., 2006). The Grave's Dock (GD) site, located within the Okatee River estuary (South Carolina), was characterized by near seawater salinity (Weston et al., 2006) and annual temperatures ranging from 15.5 to 26.8 °C. The Okatee watershed is heavily developed and nutrient inputs to the system are expected to increase in the coming years (Windom et al., 1998). Both sites had similar sediment characteristics, with sediment density in the range of ~1.1 to 1.3 g cm^{-3}, porosity in the range of 0.68–0.79, and bulk organic matter content (as loss on ignition) in the range of 5–10%. To contrast the two study sites, we include limited data from a previously published biogeochemistry study of these sediments (Table 1; see Weston et al., 2006 for detailed methods of pore water collection and analytical methods).

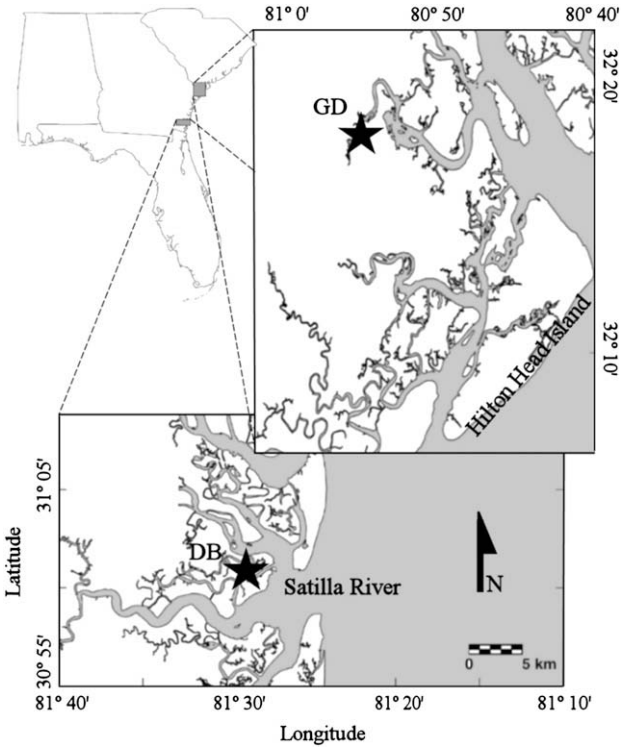

Fig. 1. Sampling locations in Georgia and South Carolina, USA. GD and DB denote Grave's Dock and Dover Bluff, respectively.

2.2. Benthic flux experimental design

Benthic fluxes were determined in re-circulating incubations of sediment cores ($n = 2$–3 cores per treatment per site). Clear acrylic core tubes with a diameter of 12 cm contained the top 20 cm of

Table 1
Integrated concentrations of pore water biogeochemical constituents in the upper 10 cm of the sediment (values taken from Weston et al., 2006). **Bold** values indicate significantly higher concentrations at DB relative to GD ($p < 0.05$).

Location	Date	NO_x[a]	NH_4^+[a]	DOC[a]	H_2S[a]	Cl^-[b]	Chl *a*[c]
DB	Jan-02	0.05	**7.37**	**63.66**	4.43	3.55	59.52
	Aug-02	0.01	**11.40**	**41.90**	**119.62**	3.78	45.53
	Jan-04	0.01	**10.34**	42.21	4.14	3.10	55.15
GD	Feb-02	n.d.	3.75	43.33	10.89	3.94	54.81
	Aug-02	0.01	2.21	31.92	4.71	3.84	56.28

[a] Units in μmol cm^{-2}.
[b] In mmol cm^{-2}.
[c] Chlorophyll concentration units are mg chl *a* m^{-2}.

sediment above which a water column of 20 cm (approximately 2.25–2.5 l) was recirculated. Creek water and intact sediment cores were collected at the same time and returned to the lab for incubation. Creek water was filtered (0.7 μm GF/F filter), and flow in the cores was maintained by re-circulating the overlying water via a peristaltic pump during the 2002 incubations; the flow speed was approximately 30 ml min^{-1}. During the 2004 incubation, the overlying water column was mixed by suspended, magnetically driven stir bars. Both methods served to limit the development of a diffusive boundary layer (adequate mixing was confirmed by dye tests).

Two incubation treatments were included for each study site and date. Dark treatments were incubated by wrapping each core in three layers of aluminum foil. Diel treatments were maintained at light levels representative of those at the sediment water interface at high tide ($2–4 \times 10^{-4}$ mol photons m^{-2} s^{-1}; as calculated from turbidity, PAR, and water column depth; data not shown) over a simulated natural diel cycle (winter: 10.5 h light, 13.5 h dark; summer: 13.5 h light, 10.5 h dark). Three different light exposure regimes were achieved using this design: "dark" (continuous darkness), "diel–day" (diel treatment during illumination), and "diel–night" (diel treatment during darkness). Flux experiments were conducted in an incubator to maintain temperatures at fixed field levels (i.e. there was no diel variation in temperature). Cores were sampled every 6–12 h for 6–14 days.

Flux experiments occurred in two phases. The first phase of the incubation determined "baseline" fluxes in diel and dark treatments. The second phase consisted of a $K^{15}NO_3^-$ amendment, which was made to the overlying water of all cores after the dark treatments became hypoxic ($[O_2] < 50$ μmol l^{-1}). Hereafter, the first phase is referred to as "baseline", and the second phase is referred to as "amended". Fluxes were calculated from the linear change in water column species concentration over time following an initial stabilization period (~24 h circulation began for baseline conditions and ~12 h following the $^{15}NO_3^-$ amendment). Fluxes into the sediment (uptake) are reported as negative numbers, while fluxes out of the sediment (release) are reported as positive numbers. Statistical comparisons of concentrations and rates between treatments were obtained by analysis of variance (ANOVA).

2.3. Sample collection

At each time point a water sample was collected via in-line syringe, and aliquots were dispensed into different vials for a variety of analyses. The volume removed, approximately 100 ml or 4% of the total volume per time point, was replaced with time zero, filtered creek water from a reservoir. Dissolved O_2 concentration and pH were determined immediately by a galvanic dissolved O_2 probe and a combination pH/reference electrode respectively. H_2S samples were fixed immediately with 500 μL of 20% zinc acetate and concentrations were determined colorimetrically (Cline, 1969).

Dissolved inorganic carbon (DIC) concentration was determined using a Shimadzu GC-14A gas chromatograph equipped with a methanizer and a flame ionization detector in January/February 2002. For the August 2002 and the January 2004 experiments, DIC concentrations were determined on a Shimadzu (TOC-5000) infrared carbon analyzer.

A 30 ml sub-sample was collected and immediately filtered (0.2 μm) into a high density polyethylene bottle and stored at 4 °C for subsequent determination of ammonium, nitrate + nitrite (NO_x), nitrite, and total dissolved nitrogen (TDN). A 5 ml sub-sample was preserved with 200 μl of phenol and NH_4^+ concentration was quantified using the phenol-hypochlorite method (Solorzano, 1969). Concentrations of NO_x and NO_2^- were determined by vanadium reduction and NO detection (Antek 745 NO_3^-/NO_2^- reduction assembly and 7050 NO detector). TDN was determined using a Shimadzu TOC-5000 coupled to an Antek 7050 NO detector (Álvarez-Salgado and Miller, 1998). Dissolved organic nitrogen (DON) was determined by difference ($DON = TDN - (NO_x + NH_4^+)$). DOC was measured on an acidified sub-sample (stored at 4 °C) using a Shimadzu TOC-5000 analyzer. After the experiment, triplicate samples were collected from each core for chlorophyll *a* quantification via 24 h extraction in 100% acetone and subsequent spectrophotometric analysis (Strickland and Parsons, 1972).

2.4. ^{15}N addition experiments

^{15}N amendments were used to determine the fate of NO_3^- in the sediment via both dissimilatory and assimilatory pathways. The water column of all cores was amended with 99 atom % $K^{15}NO_3^-$ to a final concentration of ~100 μmol l^{-1}, and the $^{15}NO_3^-$ was tracked into the N_2 pool by measuring the $^{29}N_2$ and $^{30}N_2$ masses using a membrane inlet mass spectrometer (MIMS, Kana et al., 1998; Eyre et al., 2002). The isotope pairing technique (IPT; Nielsen, 1992) was used to estimate the amount of DNF that occurred without NO_3^- amendment (D_{14}) and denitrification of the added $^{15}NO_3^-$ (D_{15}) was estimated from the amount of ^{15}N in the N_2 pool.

Production of $^{29}N_2$ in August 2002 motivated an examination of the contribution of anammox to NO_3^- consumption. In order for DNF to produce $^{29}N_2$, one $^{15}NO_3^-$ and one $^{14}NO_3^-$ would be consumed. The total available $^{14}NO_x$ was determined by adding the mean measured NO_x concentration in the overlying water of the sediment cores for each site prior to the $^{15}NO_3^-$ amendment (0.23 μmol l^{-1} NO_x for DB and 0.24 μmol l^{-1} NO_x for GD) and the amount of NO_3^- in the tracer amendment (99% $^{15}NO_3^-$ and 1% $^{14}NO_3^-$ giving 0.74 μmol l^{-1} $^{14}NO_3^-$ in the addition for DB and 1.02 μmol l^{-1} $^{14}NO_3^-$ for GD). Given the low pore water NO_3^- concentration observed in the surface sediments under *in situ* conditions (0.7–2.4 μmol l^{-1}), that the sediments were anoxic, and that DNF, as well as microbial NO_3^- assimilation, were active during the previous 4 days of incubation, it is unlikely that any pore water $^{14}NO_3^-$ remained during the amended portion of the incubation. The total amount of $^{14}NO_x$ following the amendment could account for no more than 0.97 (DB) to 1.26 (GD) μmol l^{-1} $^{29}N_2$. Excess $^{29}N_2$ above that amount thus serves as a minimum estimate of anammox activity, reflecting the conversion of $^{15}NO_2^-$ and $^{14}NH_4^+$ to $^{29}N_2$.

For the August 2002 and January 2004 experiments, the amount of $^{15}NH_4^+$ produced during the incubation was quantified at the termination of the experiment using the ammonium diffusion method (Holmes et al., 1998). DNRA rates were determined by calculating the amount of NH_4^+ produced following the $^{15}NO_3^-$ amendment and multiplying that by the ^{15}N-labeled fraction of NH_4^+ (determined from the atom % ^{15}N of the final NH_4^+ pool), which corrected for any production of $^{14}NH_4^+$ from organic matter remineralization. The resulting $^{15}NH_4^+$ concentration was compared to the $^{15}NH_4^+$ concentration prior to the ^{15}N amendment (calculated from the measured NH_4^+ concentration and ^{15}N natural abundance), to determine a DNRA rate of $^{15}NO_3^-$ (Porubsky et al., 2008).

2.5. Slurry experiment

Intact sediment cores (30 cm in depth) collected from each site ($n = 10$ per site) in December 2005 were sectioned in an anaerobic chamber under an N_2 (~97%) and H_2 (~3%) atmosphere. A 2 ml sample of wet sediment was collected for characterization of physical properties. Sediment from two depth intervals, 0–3 and 8–13 cm, was used in laboratory experiments. Artificial salt water (ASW) was used for all incubations with a salinity of 19.4 (equivalent to field salinities) and was NH_4^+- and SO_4^{2-}-free, which allowed us to

detect low levels of NH_4^+ production and to eliminate H_2S produced by sulfate reduction. Slurry incubations were performed at 23 °C.

Sediments were washed five times in the anaerobic chamber in a 4:1 (ASW:sediment) ratio prior to the onset of each experiment (Weston and Joye, 2005). Five wash cycles lowered the dissolved NH_4^+, SO_4^{2-} and H_2S concentrations to below 10 μmol l^{-1} and NO_x to below 0.5 μmol l^{-1} (data not shown). Washed sediment was combined with ASW in a 1:4 ratio and purged with 0.9% Ar in a balance of N_2 for 30 min. After purging, 16 ml aliquots of the slurry were placed into glass tubes, which were sealed without a headspace. Samples were then amended with the appropriate substrate additions, and the incubation began.

Time series incubations were conducted to determine the optimum incubation time to ensure linear rates and no substrate limitation (data not shown). The influence of H_2S on NO_3^- reduction was examined by the addition of a range of H_2S concentrations (0–5000 μmol l^{-1}) in combination with $^{15}NO_3^-$ (as a substrate for DNF and DNRA) and acetate (to prevent carbon limitation); the H_2S treatments were pH adjusted to approximately 7.25 (typical pH value for pore water in the top 20 cm, data not shown) following H_2S addition. The influence of the DOC to electron acceptor (i.e. NO_3^-) ratio was examined by addition of $^{15}NO_3^-$ and various concentrations of acetate. Time zero incubations were killed immediately by injection of $ZnCl_2$; all other samples were gently shaken for 6 h, prior to centrifugation at 400 rpm for 10 min and subsequent sampling.

Species quantification for the incubation experiments used the same analytical methods as described above for the benthic flux samples except where noted below. Following the initial sub-sampling, the three isotopic species of N_2 and the N_2:Ar ratio were quantified on the MIMS by inserting the inlet tube of the MIMS directly into the incubation tube taking care to prevent sediment from being drawn into the inlet. A 1 ml sub-sample of sediment was collected for determination of exchangeable NH_4^+ (modified from Mackin and Aller, 1984; Morin and Morse, 1999). An additional 1 ml sub-sample was collected and injected into a He-purged, crimp-sealed 8 ml headspace vial (preserved with a NaOH pellet) for determination of nitrous oxide (N_2O) concentrations via gas chromatography (Joye and Paerl, 1994). Rates were calculated as the change in concentration over time.

3. Results

3.1. Sediment biogeochemistry

Benthic chl *a* concentrations were similar at both sites on all sampling dates (range 45–56 mg chlorophyll *a* m^{-2}; Table 1); pore water salinities were not significantly different between the sampling dates. Integrated pore water inventories (upper 10 cm) for NO_3^-, NH_4^+, DOC, and salt (Cl^-), for DB and GD sites in January 2002 and August 2002 are shown in Table 1 (Weston et al., 2006). Inventories of NO_3^- were similar for both sites while NH_4^+, H_2S and DOC inventories were always higher at DB (Weston et al., 2006)

3.2. Oxic benthic fluxes

3.2.1. Baseline conditions

Baseline (prior to $^{15}NO_3^-$ addition) O_2 concentrations showed a strong diel cycle, with O_2 production during the day and O_2 consumption at night (Figs. 2A and 3A; Table 2). The O_2 concentration remained above 150 μmol l^{-1} under baseline conditions in the diel treatments. Oxygen fluxes in diel treatments indicated net autotrophy, while O_2 fluxes observed in dark treatments indicated net heterotrophy (Table 2). Baseline NO_3^- fluxes were low at both sites on all dates (Figs. 2C and 3C; Table 2). Sediments were a NO_3^- sink under diel–day and diel–night conditions, with the exception of diel–night fluxes at DB in January 2002 and diel–night fluxes at GD in February 2002 (Table 2). Concentrations of NH_4^+ decreased

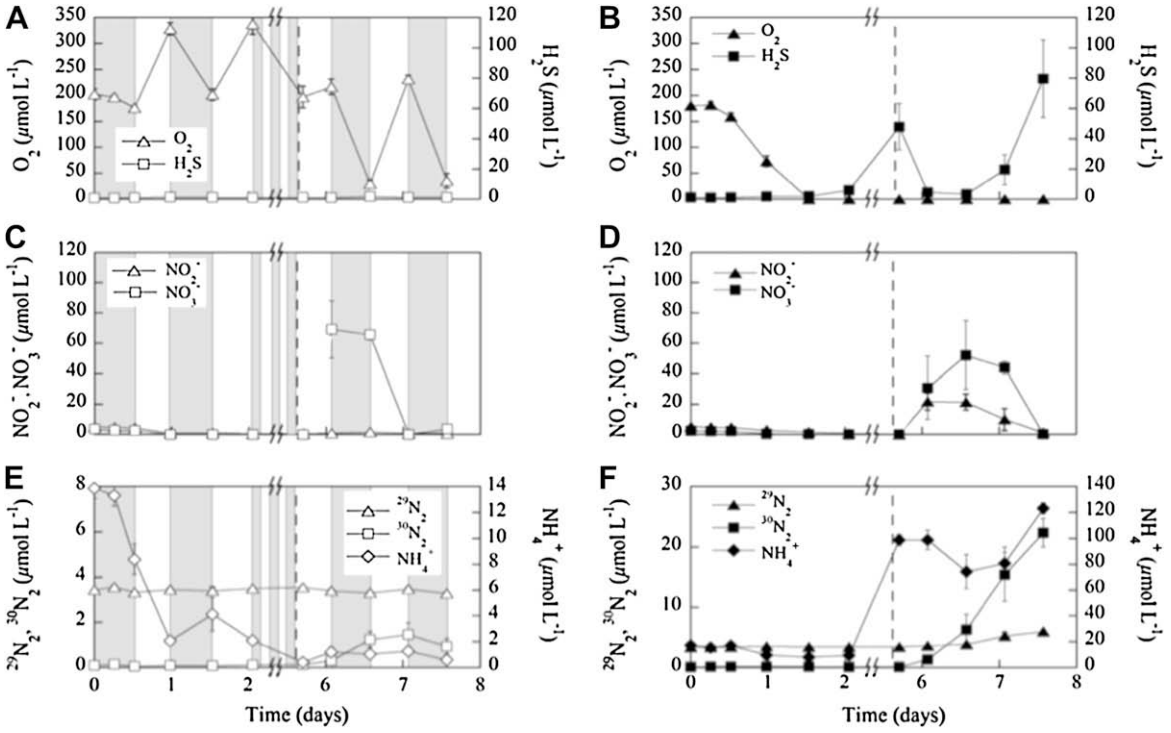

Fig. 2. (A–F). Flux core determined temporal changes in the concentration of O_2, H_2S, NO_2^-, NO_3^-, $^{29}N_2$, $^{30}N_2$ and NH_4^+, for Dover Bluff, August 2002. Left and right panels indicate diel and dark treatments, respectively; gray boxes in the left panels indicate periods of darkness. Note *x*-axis has been contracted to better illustrate the post-amendment conditions. Vertical dashed-line indicates $^{15}NO_3^-$ amendment, error bars = ± 1 SE ($n = 3$).

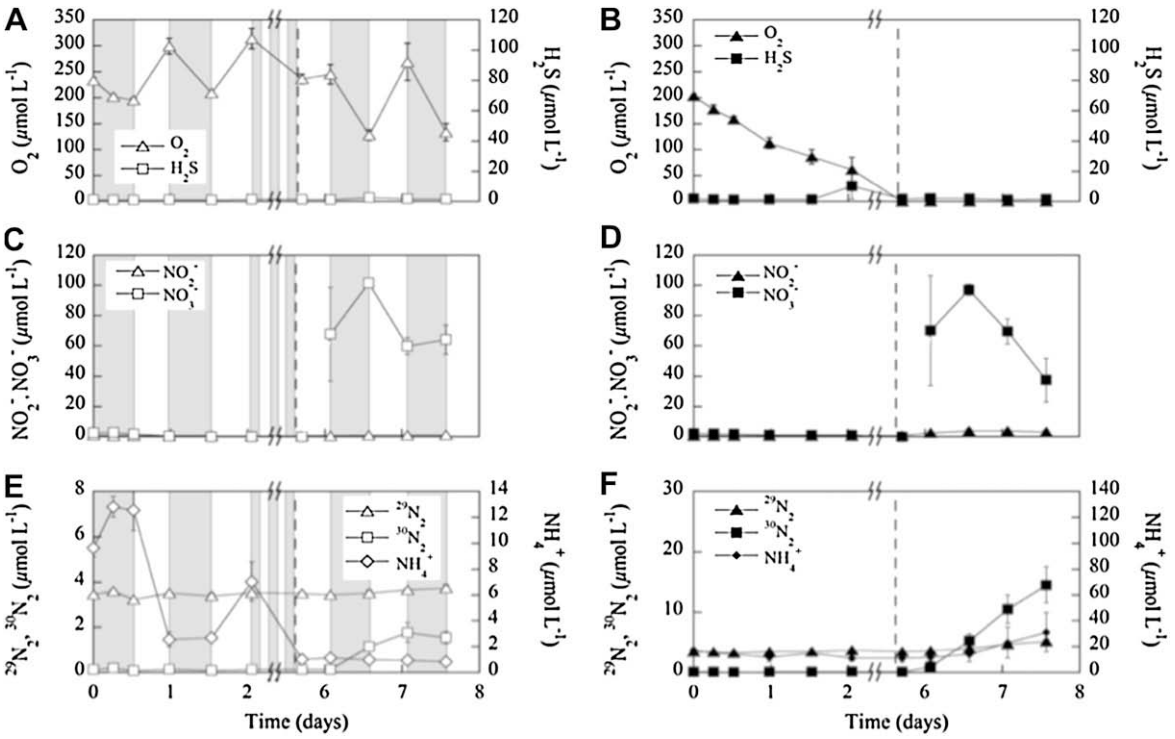

Fig. 3. (A–F) Flux core determined temporal changes in the concentration of O_2, H_2S, NO_2^-, NO_3^-, $^{29}N_2$, $^{30}N_2$ and NH_4^+, for Grave's Dock, August 2002. Left and right panels indicate diel and dark treatments, respectively; gray boxes in the left panels indicate periods of darkness. Note *x*-axis has been contracted to better illustrate the post-amendment conditions. Vertical dashed-line indicates $^{15}NO_3^-$ amendment, error bars = ± 1 SE ($n = 3$).

quickly in baseline diel treatments, usually under diel–day conditions and under diel–night conditions on several occasions (Table 2). Dissolved organic N was released under baseline diel–day conditions and taken up under diel–night conditions (Table 2). Fluxes of DOC were higher at DB than GD (Table 2).

3.2.2. Amended conditions

Following the $^{15}NO_3^-$ amendment, the absolute magnitude of O_2 fluxes increased (with the exception of winter 2002; Table 2). Amended O_2 production for August 2002 was approximately 1.3 times higher than the corresponding baseline rates under diel–day conditions (Table 2). Under diel–night conditions, amended O_2 uptake rates were approximately 1.3–2 times higher than baseline rates (Table 2). During the August experiment, O_2 production (diel–day) and consumption (diel–night) were stimulated to comparable levels and DIC fluxes showed a similar increase under diel–night conditions (Table 2). A different response to the $^{15}NO_3^-$ amendment was observed at DB in January 2004. Amended O_2 release rates under diel–day conditions were approximately 1.6-fold higher than baseline rates while diel–night O_2 consumption rates decreased (Table 2); DIC uptake under diel–day conditions exceeded DIC release rates under diel–night conditions (Table 2).

Following the $^{15}NO_3^-$ amendment, NO_3^- concentrations decreased quickly, with highest NO_3^- uptake rates usually observed under diel–day conditions, followed usually by dark conditions, and finally diel–night conditions (Figs. 2C and 3C; Table 2). Following the $^{15}NO_3^-$ amendment, fluxes of NH_4^+ remained low in diel treatments (Figs. 2E and 3E; Table 2). Fluxes of DOC increased following $^{15}NO_3^-$ addition at both sites (Table 2), and DOC release (net production) was observed during diel–day incubations.

3.2.3. DNF rates

Rates of D_{14} under diel conditions were generally low for both sites on all dates, with rates ranging from 0 to 5 μmol N m^{-2} h^{-1} (Table 3). Lower D_{14} rates correlated with lower temperatures (February 2002 GD; and January 2004 both sites). In incubations with warmer temperatures, D_{14} rates in diel incubations were lower than the corresponding rates in dark incubations. Rates of D_{15} increased by an order of magnitude in diel treatments following the $^{15}NO_3^-$ amendment (Table 3); D_{15} rates were ~4 to 13 times higher than the corresponding D_{14} rates (Table 3).

3.3. Hypoxic/anoxic benthic fluxes

3.3.1. Baseline conditions

Under dark conditions, O_2 concentrations decreased from 200 μmol L^{-1} to <50 μmol L^{-1} within about two days at both sites in August 2002 (Figs. 2B and 3B) and at DB in January 2002 (data not shown). Though baseline dark NO_3^- fluxes were low (Figs. 2D and 3D; Table 2), sediments were a consistent sink for NO_3^-. Concentrations of NH_4^+ decreased initially under baseline dark conditions but then increased under hypoxic conditions (Figs. 2F and 3F).

3.3.2. Amended conditions

Nitrate uptake rates in dark incubations increased following the $^{15}NO_3^-$ amendment (Figs. 2D and 3D; Table 2) with dark uptake rates usually being lower than diel–day uptake rates, but higher than diel–night rates (Table 2). Ammonium release rates under amended dark conditions increased up to 14 times in the August 2002 DB experiments (Table 2).

3.3.3. DNF rates

Rates of D_{14} under dark conditions were low for all sampling dates, with rates ranging from ~0 to 15 μmol N m^{-2} h^{-1} (Table 3). D_{14} rates were significantly higher under dark conditions ($p < 0.01$), and summer rates were higher than winter rates. Following the $^{15}NO_3^-$ amendment, D_{15} rates were ~15 to 45 times higher than the

Table 2
Benthic flux rates for Dover Bluff (DB) and Grave's Dock (GD). Mean rates in μmol m^{-2} h^{-1}, *n* indicates the number of time periods considered in the mean, and numbers in parentheses are ±1 standard error. 'Cores *n*=' indicates the number of diel and dark cores for each experimental date. '0 NO_3^-' and '100 NO_3^-' indicate the amount of NO_3^- added (μmol L^{-1}; i.e. baseline and amended rates, respectively).

Date	Treatment	Tracer	*n*	NO_x	NH_4^+	O_2	DIC	DOC	DON
January 2002 (DB)	Diel–day	0 NO_3^-	2	−21 (5.9)	−63 (32)	2900 (670)	−7900 (1500)	930 (290)	810 (310)
Cores *n* = 2	Diel–night		2	0.6 (5.5)	−38 (27)	−540 (79)	2900 (1300)	−960 (480)	−770 (380)
	Dark		7	−5.5 (4.7)	−7.4 (25)	−470 (79)	−130 (630)	−180 (190)	110 (260)
	Diel–day	100 NO_3^-	2	−420 (48)	2.3 (2.3)	−2200 (40)	2900 (720)	–	96 (49)
	Diel–night		2	−640 (110)	−24 (3.0)	−880 (240)	3200 (180)	–	48 (55)
	Dark		4	−450 (140)	−25 (89)	−130 (140)	−300 (1100)	–	100 (180)
August 2002 (DB)	Diel–day	0 NO_3^-	2	−62 (34)	−76 (31)	2600 (200)	−4200 (590)	560 (180)	–
Cores *n* = 3	Diel–night		2	−16 (12)	−30 (37)	−1200 (470)	1900 (720)	−140 (100)	–
	Dark		6	−24 (7.0)	11 (41)	−540 (170)	1600 (230)	330 (110)	–
	Diel–day	100 NO_3^-	1	−1200 (45)	4.2 (4.2)	3500 (230)	−2700 (810)	1000 (270)	–
	Diel–night		1	−240 (220)	−2.1 (10)	−2400 (1500)	3600 (2200)	100 (530)	–
	Dark		4	−300 (290)	140 (200)	−30 (16)	290 (2500)	−270 (630)	–
January 2004 (DB)	Diel–day	0 NO_3^-	3	−0.9 (1.5)	−24 (8.3)	1600 (460)	−330 (370)	–	24 (53)
Cores *n* = 3	Diel–night		3	−2.8 (1.2)	1.7 (5.5)	−1100 (79)	1100 (100)	–	−34 (74)
	Dark		7	−0.1 (0.7)	48 (7.4)	−400 (82)	700 (170)	–	−13 (42)
	Diel–day	100 NO_3^-	4	−180 (8.3)	−23 (15)	2600 (250)	−1500 (240)	–	72 (18)
	Diel–night		4	−71 (9.4)	7.7 (10)	−850 (160)	670 (58)	–	−38 (17)
	Dark		8	−85 (6.6)	61 (12)	−9.3 (19)	290 (63)	–	−9.0 (23)
February 2002 (GD)	Diel–day	0 NO_3^-	2	−23 (6.8)	−6.9 (6.5)	3800 (150)	−2400 (400)	38 (72)	84 (49)
Cores *n* = 2	Diel–night		2	12 (16)	4.1 (6.8)	−2000 (380)	1500 (230)	56 (150)	−83 (80)
	Dark		5	−1.5 (2.1)	3.6 (3.7)	−400 (190)	−490 (1000)	100 (89)	−11 (45)
	Diel–day	100 NO_3^-	2	−630 (60)	8.2 (0.4)	740 (430)	420 (140)	510 (470)	150 (32)
	Diel–night		2	−380 (24)	−4.2 (2.8)	−2200 (140)	930 (200)	280 (110)	98 (54)
	Dark		5	−190 (82)	15 (6.8)	−330 (88)	730 (560)	180 (210)	52 (40)
August 2002 (GD)	Diel–day	0 NO_3^-	2	−13 (7.3)	−59 (76)	1800 (75)	−2800 (410)	310 (170)	−38
Cores *n* = 3	Diel–night		2	−18 (2.5)	26 (17)	−1000 (250)	1100 (130)	−220 (130)	–
	Dark		6	−5.8 (1.1)	−26 (19)	−540 (92)	570 (93)	57 (75)	–
	Diel–day	100 NO_3^-	1	−740 (110)	−0.9 (6.3)	2500 (410)	−1800 (1300)	880 (180)	–
	Diel–night		1	55 (200)	−4.5 (1.0)	−1300 (120)	1900 (560)	−220 (85)	–
	Dark		6	−500 (32)	150 (18)	−77 (30)	1400 (360)	260 (76)	–
January 2004 (GD)	Diel–day	0 NO_3^-	3	−2.2 (1.2)	−1.6 (6.9)	1500 (400)	−890 (290)	–	230 (110)
Cores *n* = 3	Diel–night		3	−2.0 (2.9)	−16 (9.5)	−770 (41)	680 (90)	–	−47 (56)
	Dark		7	−0.6 (1.2)	−6.1 (7.1)	−330 (42)	260 (46)	–	54 (52)
	Diel–day	100 NO_3^-	4	−200 (25)	3.1 (8.8)	2300 (180)	−1800 (240)	–	5.9 (20)
	Diel–night		4	−80 (9.3)	−6.0 (8.1)	−620 (180)	−380 (1000)	–	9.5 (13)
	Dark		7	−60 (6.2)	42 (22)	−30 (30)	120 (78)	–	−16 (24)

Table 3
Denitrification rates for DB and GD on several dates. Units are μmol N m^{-2} h^{-1}, *n* is the number of replicates and numbers in parentheses are ±1 standard error. Stats indicate significant ($p < 0.05$) differences between the following: *a*, D_{14} and D_{15}; *b*, dark D_{14} and diel D_{14}; *c*, dark D_{15} and diel D_{15}; *d*, DB and GD for a given value.

January 2002					
DB	D_{14}	D_{15}	GD	D_{14}	D_{15}
Dark (*n* = 2)	5.36 (1.67)	98.54 (9.85)	Dark (*n* = 2)	0.73 (0.04)	18.93 (1.05)
stats	*a*	*a,c*	stats	–	–
Diel (*n* = 2)	2.38 (0.60)	10.36 (3.79)	Diel (*n* = 2)	0.74 (0.33)	9.88 (4.90)
stats	–	*c*	stats	–	–
August 2002					
DB	D_{14}	D_{15}	GD	D_{14}	D_{15}
Dark (*n* = 3)	15.74 (0.72)	280.30 (26.72)	Dark (*n* = 3)	9.66 (1.87)	166.04 (37.34)
stats	*a,b,d*	*a,c*	stats	*d*	
Diel (*n* = 2)	1.32 (0.00)	29.87 (5.21)	Diel (*n* = 2)	4.17 (1.16)	24.28 (0.97)
stats	*b*	*c*	stats	–	
January 2004					
D_{14}	D_{15}	GD	D_{14}	D_{15}	D_{14}
Dark (*n* = 3)	0.50 (0.05)	23.34 (3.88)	Dark (*n* = 3)	0.51 (0.23)	14.13 (3.49)
stats	*a*	*a*	stats	*a*	*a*
Diel (*n* = 3)	0.87 (0.25)	14.01 (3.23)	Diel (*n* = 2)	0.00 (0.13)	7.00 (1.88)
stats	*a*	*a*	stats	–	

D_{14} rates (Table 3). Dark D_{15} rates were significantly higher than diel D_{15} rates at DB in January 2002 ($p < 0.01$) and at both sites in August 2002 ($p < 0.05$; Table 3).

3.4. Dissimilatory NO_3^- sinks

Results from the DB dark experiment in August 2002 illustrated the complex interactions that can result from sudden increases in water column NO_3^- concentration. Prior to the $^{15}NO_3^-$ amendment, the concentration of NH_4^+ had increased to 100 μmol l^{-1} (Fig. 2F). The amendment increased the NO_3^- concentration from 0.23 to 73.6 μmol l^{-1}. Afterwards, NO_2^- concentration increased from 0.56 to 21.7 μmol l^{-1}. Then, NO_2^- concentration decreased to 1.2 μmol l^{-1}, and the NH_4^+ concentration decreased to 74.4 μmol l^{-1} (Fig. 2D). The stoichiometry of NH_4^+ and NO_2^- uptake was approximately 1:1. Concentrations of $^{29}N_2$ increased concomitantly with the decrease in NO_2^- and NH_4^+ concentrations. $^{30}N_2$ concentrations increased from baseline levels to approximately 22 μmol l^{-1} following the $^{15}NO_3^-$ amendment (Fig. 2F).

After the NO_2^- concentration declined to 1.2 μmol l^{-1}, the NH_4^+ concentration increased to 123 μmol l^{-1} (Fig. 2F). The atom % ^{15}N of the NH_4^+ pool (6.9 atom % ^{15}N at DB) indicated a minimum production of 8.4 μmol l^{-1} $^{15}NH_4^+$ via DNRA, which amounted to 11.4% of the $^{15}NO_3^-$ amendment. This value may be an underestimate as it does not include $^{15}NH_4^+$ that may have been produced and subsequently

utilized via anammox ($^{15}NO_2^- + {}^{15}NH_4^+ = {}^{30}N_2$) or $^{15}NH_4^+$ that may have sorbed onto the sediment. The rate of DNRA at DB in August 2002 was 38 μmol N m^{-2} h^{-1}, which amounts to 13.5% of the D_{15} rate (~280 μmol N m^{-2} h^{-1}) for the dark treatment (Table 3).

3.5. Slurry experiments

The influence of H_2S concentration on NO_3^- reduction was investigated by addition of $^{15}NO_3^-$ and one of four H_2S concentrations (0, 20, 500, or 5000 μmol H_2S l^{-1}; Fig. 4A–D). Higher H_2S concentrations correlated with lower NO_3^- consumption rates and less NO_2^- accumulation (Fig. 4A and B). There was no correlation between NH_4^+ concentration and H_2S concentration. Even at a lower (20 μmol l^{-1}) H_2S concentration, the percentage of N_2O relative to N_2 production increased (Fig. 4C and D) from 22 to 83% at DB and from 9 to 36% at GD (Fig. 4C and D). The total products of DNF from the $^{15}NO_3^-$ addition ($2 \times ([N_2O] + [^{30}N_2]) + 1 \times [^{29}N_2]$) decreased as H_2S concentration increased in the 0–3 cm depth at both sites (Fig. 4C and D).

The influence of the DOC:NO_3^- ratio on NO_3^- reduction rates and pathways was examined by the addition of 50 μmol $^{15}NO_3^-$ l^{-1} and various concentrations of acetate (0–10,000 μmol C l^{-1}; Fig. 5A–D) to DB surface (0–3 cm) sediments. The NO_3^- concentration decreased similarly and significantly ($p < 0.05$, data not shown) in all treatments. Significant ($p < 0.05$) increases in NH_4^+ concentration occurred only at DOC concentrations ≥7500 μmol l^{-1}. Concentrations of N_2O increased significantly with increasing DOC concentration up to the 2500 μmol DOC l^{-1} treatment. The concentration of $^{30}N_2$ exhibited a similar pattern to N_2O with significant ($p < 0.05$) increases in all treatments; however, $^{30}N_2$ concentration decreased significantly ($p < 0.05$) with increasing DOC:NO_3^- ratio between 1000 and 7500 μmol DOC l^{-1}.

The DOC:NO_3^- ratio did not significantly affect the consumption of NO_3^- but led to differences in the end products of DNF, with N_2O comprising a larger portion of the DNF production with increasing DOC:NO_3^- ratio (Fig. 5A). The total rate of DNF ($N_2O + {}^{15}N\text{–}N_2$) decreased and the NH_4^+ concentration increased as the DOC:NO_3^- ratio increased (Fig. 5B). The ratio of the rates of DNRA to DNF was influenced by the DOC:NO_3^- ratio (Fig. 5C).

4. Discussion

4.1. Light level, the balance of autotrophy and heterotrophy, and influence of BMA on biogeochemical cycling

Light levels are correlated with the net metabolic state of shallow sediments (Cabrita and Brotas, 2000). Large diel variations in O_2 flux have been reported in the literature (−5000 to 6000 μmol O_2 m^{-2} h^{-1}; Cabrita and Brotas, 2000; Sundbäck et al., 2000) and baseline O_2-based primary production rates for the current study (Table 2) fell within the range typical of active sediments. Net O_2 production rates in the diel–day treatment were ~2 times higher than O_2 uptake at night, indicating net autotrophy. Dark treatments became hypoxic within 24–48 h and ultimately became anoxic (Figs. 2B and 3B). Anoxic conditions resulted in significant changes in the fluxes of nutrients and dissolved gases across the sediment water interface. Though the metabolic rates could have been impacted by the incubation duration, the N amendment had a larger impact.

Extended periods of decreased light availability in the benthos can result from storm runoff, which leads to higher turbidity. In addition to storm-induced turbidity, coastal eutrophication, driven by anthropogenic nutrient loading (Nixon, 1995), has increased the frequency and spatial coverage of water column algal blooms (Paerl et al., 2003). Increased turbidity resulting from algal blooms leads to light limitation of the benthos, which generates hypoxic/anoxic conditions and affects benthic fluxes. Furthermore, as algal blooms decline bottom water and sediment metabolism are stimulated (Paerl et al., 2003). Such events lead to dramatic changes to the already fragile balance of heterotrophy and autotrophy in coastal ecosystems (Steward et al., 2006).

Inorganic nutrient availability also impacted the flux of dissolved organics. DOC release increased during the diel–day period following the N amendment. Though DOC uptake in the diel–night increased as well, daytime release of DOC outpaced nighttime uptake. Some diatom species release between ~5 and 20% of the total C fixed as DOC (Wetz and Wheeler, 2007). BMA-derived DOC efflux can occur as simple exudation of excess production as DOC during times of nutrient limitation when cellular C:N ratios are

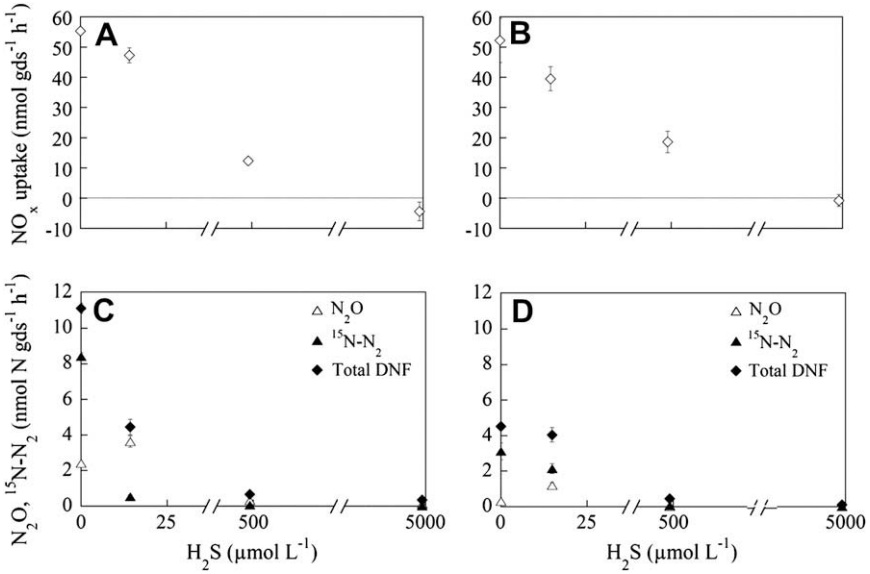

Fig. 4. (A–D) Nitrogen cycling rates from sulfide manipulation experiments for DB 0–3 cm (A and C) and GD 0–3 cm (B and D). Note compression of the *x*-axis in all panels. The $^{15}N\text{–}N_2$ rate corresponds to the $^{29}N_2$ production rate plus 2 times the $^{30}N_2$ production rate; total DNF is the sum of the N_2O and $^{15}N\text{–}N_2$ production rates in terms of N. Error bars are ±1 SE ($n = 3$).

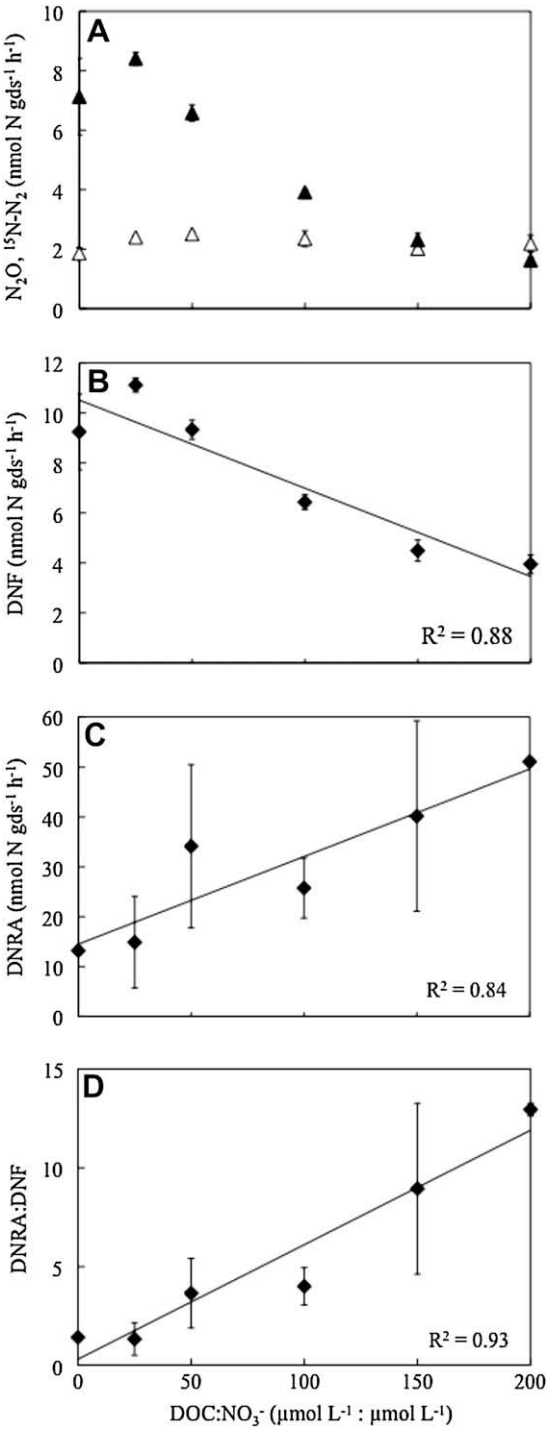

Fig. 5. (A–D) Nitrogen cycling rates for DOC:NO_3^- ratio manipulation experiments for DB 0–3 cm. Trend lines represent linear relationships. DNF is the sum of the N_2O and ^{15}N–N_2 production rates in terms of N; DNRA is the production rate of total NH_4^+ (NH_4^+ DISS + NH_4^+ ADS). Error bars are ±1 SE ($n = 3$).

unfavorable (Cook et al., 2004). Bacteria have been shown to rapidly assimilate DOC released by BMA (Jensen, 1984) and microalgal and heterotrophic processes are often tightly coupled (Joye et al., 1996). Here, DOC production by BMA exceeded the bacterial consumption typically observed in benthic systems. This nutrient-stimulated decoupling of organic matter (OM) production and consumption in the benthos could be intensified by short-term nutrient inputs which satiate BMA with DIN (Porubsky et al., 2008).

4.2. Denitrification

NO_3^- availability can regulate rates and pathways of N processing in sediments. Unamended DNF rates determined using similar techniques at other sites ranged from 8 to 330 µmol N m^{-2} h^{-1} (An and Gardner, 2002; An et al., 2001; Risgaard-Petersen et al., 2004). The maximum D_{14} rates for the current study were 20 µmol N m^{-2} h^{-1}. Denitrification proceeds by direct reduction of NO_3^- supplied from the water column or by coupling to nitrification within the sediment (hereafter 'coupled DNF', Nishio et al., 1983). NO_3^- limitation of DNF can be induced by low water column NO_3^- concentrations or by substrate limitation of nitrification (Seitzinger, 1994). Water column NO_3^- concentrations in the creek were low at both sites (1.6 µmol l^{-1} at DB and 2.2 µmol L^{-1} at GD; Joye, unpublished data) and likely limit DNF. NH_4^+ limitation of nitrification has been reported for NH_4^+ concentrations in the range of 70–700 µmol L^{-1} (Henrikson and Kemp, 1988). Though NH_4^+ concentrations in surficial sediments were on the order of 50 µmol l^{-1}, pore water NH_4^+ concentrations at 15 cm reached mmol l^{-1} concentrations (Weston et al., 2006). This upwardly diffusing NH_4^+ source could support substantial nitrification activity. No nitrification would have occurred in the dark incubations since the cores were anoxic and no anaerobic nitrification coupled to manganese oxide reduction (Hulth et al., 1999) was observed.

During times of active BMA photosynthesis, the vertical extent of the oxic zone increases, which can lead to higher volumetric rates of nitrification and coupled DNF (Rysgaard et al., 1993). However, at the same time, BMA compete with nitrifiers and denitrifiers for NH_4^+ and NO_3^- respectively, which could further exacerbate NO_3^- limitation of DNF (Rysgaard et al., 1993; Cabrita and Brotas, 2000; An and Joye, 2001). Rates of D_{14} were relatively low in diel and dark treatments (Table 3), likely due to NO_3^- limitation driven primarily by competition for NO_3^- with phototrophs in the former case and by extremely low nitrification (and resulting low NO_3^- concentration) in the latter case.

Low D_{14} rates at the anthropogenically impacted DB site could also result from inhibition of coupled DNF by the high pore water H_2S concentrations (Table 1; Joye and Hollibaugh, 1995; Weston et al., 2006). Sulfide inhibits primarily the first step of nitrification (Joye and Hollibaugh, 1995), and even lower H_2S concentrations (20 µmol l^{-1}) directly inhibit DNF (Joye, 2002).

The NO_3^- amendment led to increased rates of D_{15} that were similar to rates reported at other sites (An and Gardner, 2002; An et al., 2001; Risgaard-Petersen et al., 2004). Rates of D_{15} in dark treatments were significantly ($p < 0.05$) higher than rates in diel treatments for DB in January and August 2002 (Table 3). We hypothesize that under diel–day conditions BMA out competed denitrifiers for the added NO_3^-. Increased BMA production, and subsequent deeper O_2 penetration depths, increased NO_3^- diffusion distances and further separated denitrifiers from their substrate (Rysgaard et al., 1993). Even if anoxic microzones were present within the oxic zone, deeper O_2 penetration depths would impact the volume and location of the microzones, and thus impact DNF rates. Furthermore, denitrifiers are also capable of aerobic respiration (a process that yields more energy than DNF), and under sufficient O_2 concentrations, denitrifiers are likely to use aerobic respiration instead of DNF (Payne, 1981).

4.3. Competition between dissimilatory nitrate reduction pathways

Under dark conditions, microorganisms compete with each other for available NO_3^- In the current study, under amended conditions, D_{15} rates were 166 and 280 µmol N m^{-2} h^{-1} for GD and DB, respectively, in August 2002; while DNRA rates were 23 and 38 µmol N m^{-2} h^{-1}. DNRA comprised about 11% of the dissimilatory

NO_3^- reduction at each site. The factors that control the balance of DNF and DNRA are poorly constrained and several possible regulatory scenarios have been suggested.

Temperature may influence partitioning between dissimilatory NO_3^- reduction pathways. Previous studies showed DNF was the dominant process for NO_3^- reduction at low temperatures (<10–12 °C), and DNRA became dominant at higher temperatures (≥20 °C; Ogilvie et al., 1997). The temperatures for our experiments ranged from 15.5 to 20.5 °C in winter and 21.1 to 28.6 °C in summer. Winter temperatures were never in the range favoring DNF, and summer temperatures were always in the range favoring DNRA (Ogilvie et al., 1997). Our results indicate that DNRA remained of secondary importance relative to DNF throughout the year. Differential O_2 controls have also been hypothesized to influence the relative importance of DNF and DNRA (Fazzolari et al., 1998) because DNRA is less sensitive to O_2 than DNF. Given the anoxic condition of the water column in the dark incubations, differential O_2 sensitivity did not influence the balance of DNF and DNRA.

Sulfide inhibits the first step of nitrification (Joye and Hollibaugh, 1995) and both the NO and N_2O reductase of denitrifying bacteria (Sørensen et al., 1980). Alternatively, H_2S can stimulate DNRA by acting as an electron donor for the reduction of NO_3^- to NH_4^+ (Brunet and Garcia-Gil, 1996). Sulfide concentrations may thereby influence the balance between DNF and DNRA (An and Gardner, 2002). In the slurry experiment, H_2S concentrations of 20 μmol l^{-1} led to increased accumulation of N_2O (Fig. 4C and D). In agreement with other studies showing a negative correlation between H_2S and DNF, total DNF rates in the slurry experiment decreased with increasing H_2S concentrations (Sørensen et al., 1980; Joye, 2002). However, DNRA rates did not correlate to H_2S concentration as observed previously (Brunet and Garcia-Gil, 1996).

The negative correlation between NO_3^- consumption rates and H_2S concentration suggests H_2S impacted NO_3^- reduction at the initial reductive step from NO_3^- to NO_2^-. In the 20 μmol l^{-1} H_2S treatment, 82% of the initial NO_3^- was consumed during the incubation (Fig. 5). In the 500 μmol l^{-1} treatment, the NO_3^- consumption decreased to 0 and 21% for DB and GD, respectively, and no NO_3^- consumption was observed in the 5000 μmol H_2S l^{-1} treatment. The decreased NO_3^- consumption indicates that H_2S can completely inhibit both DNF and DNRA. High pore water H_2S concentrations occur at these study sites (Table 1; Weston et al., 2006) and the range of H_2S concentrations in the winter of 2002 was 20–1000 μmol l^{-1} in surface (0–2 cm) sediments. Concentrations increased in August 2002 to 200–3000 μmol l^{-1} at the same depth. While H_2S concentrations of 20 μmol l^{-1} would not completely block DNF or DNRA, higher concentrations observed by Weston et al. (2006) at deeper depths and at different times of the year could certainly inhibit these dissimilatory processes.

Another factor previously hypothesized to regulate the importance of DNF versus DNRA is the electron donor to electron acceptor ratio (Tiedje et al., 1982; Tiedje, 1994). Although this hypothesis was not derived empirically, it has been corroborated by field studies (Bonin, 1996; Fazzolari et al., 1998). DNRA provides slightly more energy per mole of NO_3^- reduced than does DNF. Under highly reduced conditions, a lack of electron acceptors could limit growth (Tiedje et al., 1982), and since DNRA consumes more electrons than DNF, it should be more favorable. Thus, when the DOC:NO_3^- ratio is high, DNRA would be favored.

In the slurry experiments, the balance of DNF and DNRA was examined by explicitly manipulating the DOC:NO_3^- ratio. Unlike H_2S addition, DOC addition did not alter N_2O production, but the production of $^{30}N_2$ decreased substantially as DOC increased (Fig. 5A). Both DNF and DNRA rates correlated with DOC:NO_3^- ratios (Fig. 5). At high DOC:NO_3^- ratios, electron acceptor (NO_3^-) availability should limit dissimilatory NO_3^- reduction while at low DOC:NO_3^- ratios, reductant (DOC) availability may be limiting. Our results confirm the Tiedje et al. (1982) hypothesis and show a direct correlation between the DOC:NO_3^- ratio and the DNRA:DNF rate ratio (Fig. 5D).

Uncertainties regarding the mechanistic relationship between DNF and DNRA are further complicated by evidence of the anammox process (Fig. 2F). While anammox accounted for 24 and 67% of the N_2 produced in sediments from two continental shelf sites (Thamdrup and Dalsgaard, 2002), the contribution of the process in intertidal sediments has not been previously reported. The minimum relative contribution of anammox to N_2 production in our August 2002 DB incubation was about 6.4%. This is equivalent to about 2.2% of the $^{15}NO_3^-$ reduced (Fig. 2F). Accumulation of $^{29}N_2$ significantly ($p < 0.01$) exceeded the $^{29}N_2$ possibly originating from any residual $^{14}NO_3^-$. An anammox rate of 0.05 μmol m^{-2} h^{-1} is a minimum estimate because this rate is based solely on $^{29}N_2$ production. During a $^{15}NO_3^-$ tracer experiment where DNRA was also important, anammox may also produce $^{30}N_2$, but this cannot be distinguished from $^{30}N_2$ produced via DNF.

The temporary accumulation of NO_2^- observed in August 2002 (Fig. 2D) was also reported in other studies (Dalsgaard and Thamdrup, 2002; Thamdrup and Dalsgaard, 2002); these authors suggested that NO_3^- reduction to NO_2^- was coupled to organic matter oxidation, and that NO_2^- was then used to oxidize NH_4^+. We propose a similar progression of NO_3^- reduction for these sediments, with NO_2^- accumulating due to serial substrate utilization of the intermediate products (Payne, 1981). Denitrifiers possessing NO_3^- reductase reduce NO_3^- preferentially because the reduction of NO_3^- to NO_2^- confers more energy per mole N ($G^{\circ'} = -161$ kJ mol^{-1}) than the reduction of NO_2^- to NO ($G^{\circ'} = -76.2$ kJ mol^{-1}; Tiedje, 1994). After NO_3^- is depleted, NO_2^- is reduced (Payne, 1981). Some denitrifiers (and bacteria capable of anammox) may lack NO_3^- reductase, and these microbes consume accumulated NO_2^-. The accumulation of NO_3^- has been observed in ^{15}N amendment experiments that utilize a relatively high concentration of $^{15}NO_3^-$ (Dalsgaard et al., 2005). This accumulation occurred during the initial phase of the amendment, while NO_3^- was abundant, and it is likely that during this period NO_2^- was not utilized as an electron acceptor (Dalsgaard et al., 2005).

Contemporaneous DNF and anammox complicates the interpretation of data obtained using the IPT (Kartal et al., 2007). An alternative form of the IPT equation permits estimation of DNF rates in the presence of anammox (Risgaard-Petersen et al., 2003). However, in August 2002, sediments in the DB dark incubations also exhibited DNRA activity. Recent evidence indicates that anammox bacteria are capable of DNRA and can supply themselves with NH_4^+ under NH_4^+-limited conditions (Kartal et al., 2007). The same study pointed out that, under these conditions, the alternative IPT fails to account for the concomitant production of $^{30}N_2$ by DNF and anammox. In the presence of DNRA, both DNF and anammox are capable of producing all three isotopic species of N_2, so it is impossible to apply the alternative IPT equation presented by Risgaard-Petersen et al. (2003). Given that anammox has not previously been documented in intertidal creek bank sediments, multiple tracers (i.e. $^{15}NO_3^-$, $^{15}NH_4^+$) were not employed in the current study. The use of multiple tracers would have allowed for the application of the modified IPT method and for the contributions of DNF, DNRA, and anammox to be more fully examined. As our understanding of coastal nitrogen cycling increases, it is important to probe for all existing pathways and adapt the protocols accordingly.

Fluxes between the sediment and water column play an important role in estuarine nutrient cycles. Under light replete conditions, autotrophic metabolism dominated, and BMA formed an effective cap at the sediment water interface regulating the flux

of nutrients across the interface by direct uptake of nutrients and by potentially increasing the depth of the oxic zone. Under dark conditions, heterotrophic metabolism led to release of nutrients from the sediment to the water column, and dissimilatory processes dominated the nitrogen cycle. Under anoxic conditions, DNF, DNRA, and anammox competed for substrate. Although evidence for DNF, DNRA and anammox was present, the co-occurrence of all three processes (August 2002) made it impossible to determine absolute process rates or relative contributions of individual processes to total NO_3^- reduction with the use of only a single tracer. Future studies in coastal sediments should consider these three pathways of NO_3^- reduction, and additional approaches are necessary to investigate process interactions when all three processes co-occur. It appears a suite of factors (including H_2S and DOC:NO_3^-) influenced these dissimilatory processes, and though DNF was the dominant dissimilatory sink for NO_3^-, the apparent importance of DNRA and anammox illustrate the need for further detailed, process-oriented investigations into the fate of NO_3^- in coastal sediments.

Acknowledgments

We thank M. Erickson and P. Olecki for help in the field and laboratory and W. Gardner and two anonymous reviewers for providing critical comments that substantially improved this manuscript. This research was supported by the National Science Foundation's Georgia Coastal Ecosystems Long Term Ecological Research Program (OCE 99-82133 and OCE 06-20959) and National Oceanic and Atmospheric Administration Sea Grant Programs in Georgia (award numbers NA06RG0029-R/WQ11 and R/WQ12A) and South Carolina (award number: NA960PO113).

References

Aller, R., 1994. Bioturbation and remineralization of sedimentary organic matter: effects of redox oscillation. Chemical Geology 114, 331–345.

Álvarez-Salgado, X., Miller, A., 1998. Simultaneous determination of dissolved organic carbon and total dissolved nitrogen in seawater by high temperature catalytic oxidation: conditions for precise shipboard measurements. Marine Chemistry 62, 325–333.

An, S., Gardner, W., 2002. Dissimilatory nitrate reduction to ammonium (DNRA) as a nitrogen link, versus denitrification as a sink in a shallow estuary (Laguna Madre/Baffin Bay, Texas). Marine Ecology Progress Series 237, 41–50.

An, S., Gardner, W., Kana, T., 2001. Simultaneous measurement of denitrification and nitrogen fixation using isotope pairing with membrane inlet mass spectrometry analysis. Applied and Environmental Microbiology 67, 1171–1178.

An, S., Joye, S., 2001. Enhancement of couple nitrification-denitrification by benthic photosynthesis in shallow estuarine sediments. Limnology and Oceanography 46, 62–74.

Bonin, P., 1996. Anaerobic nitrate reduction to ammonium in two strains isolated from coastal marine sediment: a dissimilatory pathway. FEMS Microbiology Ecology 19, 27–38.

Brunet, R., Garcia-Gil, L., 1996. Sulfide-induced dissimilatory nitrate reduction ammonia in anaerobic freshwater sediments. FEMS Microbiology Ecology 21, 131–138.

Cabrita, M., Brotas, V., 2000. Seasonal variation in denitrification and dissolved nitrogen fluxes in intertidal sediments of the Tagus estuary, Portugal. Marine Ecology Progress Series 202, 51–65.

Cline, J., 1969. Spectrophotometric determination of hydrogen sulfide in natural waters. Limnology and Oceanography 14, 454–458.

Cook, P., Revill, A., Butler, E., Eyre, B., 2004. Carbon and nitrogen cycling on intertidal mudflats of a temperate Australian estuary. II. Nitrogen cycling. Marine Ecology Progress Series 280, 39–54.

Dalsgaard, T., Thamdrup, B., 2002. Factors controlling anaerobic ammonium oxidation with nitrite in marine sediments. Applied and Environmental Microbiology 68, 3802–3808.

Dalsgaard, T., Thamdrup, B., Canfield, D., 2005. Anaerobic ammonium oxidation (anammox) in the marine environment. Research in Microbiology 156, 457–464.

Eyre, B., Ferguson, A., 2002. Comparison of carbon production and decomposition, benthic nutrient fluxes and denitrification in seagrass, phytoplankton, benthic microalgae- and macroalgae-dominated warm-temperate Australian lagoons. Marine Ecology Progress Series 229, 43–59.

Eyre, B., Rysgaard, S., Dalsgaard, T., Christensen, P., 2002. Comparison of isotope pairing and N_2/Ar methods for measuring sediment denitrification rates – assumptions, modifications, and implications. Estuaries 25, 1077–1087.

Fazzolari, E., Nicolardot, B., Germon, J., 1998. Simultaneous effects of increasing levels of glucose and oxygen partial pressures on denitrification and dissimilatory nitrate reduction to ammonium in repacked soil cores. European Journal of Soil Biology 34, 47–52.

van de Graaf, A., Mulder, A., de Bruijn, P., Jetten, M., Robertson, L., Kuenen, J., 1995. Anaerobic oxidation of ammonium is a biologically mediated process. Applied and Environmental Microbiology 61, 1246–1251.

Henrikson, K., Kemp, W., 1988. Nitrification in estuarine and coastal marine sediments: methods, patterns and regulating factors. In: Blackburn, T., Sørensen, J. (Eds.), Nitrogen Cycling in Coastal Marine Environments, Proceedings of the SCOPE Symposium 33. John Wiley & Sons.

Holmes, R., McClelland, J., Sigman, D., Fry, B., Peterson, B., 1998. Measuring ^{15}N–NH_4^+ in marine, estuarine, and fresh water: an adaptation of the ammonia diffusion method for samples with low ammonium concentrations. Marine Chemistry 60, 235–243.

Howarth, R., Marino, R., Lane, J., Cole, J., 1988. Nitrogen fixation in freshwater, estuarine and marine ecosystems: 1. Rates and importance. Limnology and Oceanography 33, 669–687.

Hulth, S., Aller, R., Gilbert, F., 1999. Coupled anoxic nitrification/manganese reduction in marine sediments. Geochimica et Cosmochimica Acta 63, 49–66.

Jahnke, R., Nelson, J., Marinelli, R., Eckman, J., 2000. Benthic flux of biogenic elements on the Southeastern US continental shelf: influence of pore water advective transport and benthic microalgae. Continental Shelf Research 20, 109–127.

Jensen, L., 1984. Antimicrobial action of antibiotics on bacterial and algal carbon metabolism: on the use of antibiotics to estimate bacterial uptake of algal extracellular products (EOC). Archive Fur Hydrobiologie 99, 423–432.

Joye, S., 2002. Denitrification in the marine environment, p. 1010–1019. In: Collins, G. (Ed.), Encyclopedia of Environmental Microbiology. John Wiley & Sons, Inc.

Joye, S., Hollibaugh, J., 1995. Sulfide inhibition of nitrification influences nitrogen regeneration in sediments. Science 270, 623–625.

Joye, S., Mazzotta, M., Hollibaugh, J., 1996. Community metabolism in microbial mats: the occurrence of biologically mediated iron and manganese reduction. Estuarine, Coastal and Shelf Science 43, 747–766.

Joye, S., Paerl, H., 1994. Nitrogen cycling in marine microbial mats: rates and patterns of nitrogen fixation and denitrification. Marine Biology 119, 285–295.

Kana, T., Sullivan, M., Cornwell, J., Groszkowski, K., 1998. Denitrification in estuarine sediments determined by membrane inlet mass spectrometry. Limnology and Oceanography 43, 334–339.

Kartal, B., Kuypers, M., Lavik, G., Schalk, J., Op den Camp, H., Jetten, M., Strous, M., 2007. Anammox bacteria disguised as denitrifiers: nitrate reduction to dinitrogen gas via nitrite and ammonium. Environmental Microbiology 9, 635–642.

Koike, I., Hattori, A., 1978. Simultaneous determinations of nitrification and nitrate reduction in coastal sediments by a ^{15}N dilution technique. Applied and Environmental Microbiology 25, 853–857.

Mackin, J., Aller, R., 1984. Ammonium adsorption in marine sediments. Limnology and Oceanography 29, 250–257.

Morin, J., Morse, J., 1999. Ammonium release from resuspended sediments in the Laguna Madre estuary. Marine Chemistry 65, 97–110.

Nielsen, L., 1992. Denitrification in sediment determined from nitrogen isotope pairing. FEMS Microbiology Letters 86, 347–362.

Nishio, T., Koike, I., Hattori, A., 1983. Estimates of denitrification and nitrification in coastal and estuarine sediments. Applied and Environmental Microbiology 45, 444–450.

Nixon, S., 1995. Coastal marine eutrophication: a definition, social causes, and future concerns. Ophelia 41, 199–219.

Nixon, S., Oviatt, C., Hale, S., 1976. Nitrogen regeneration and the metabolism of coastal marine bottom communities. In: Anderson, J., Macfadyen, A. (Eds.), The Role of Terrestrial and Aquatic Organisms in Decomposition Processes. Blackwell, pp. 269–283.

Ogilvie, B., Rutter, M., Nedwell, D., 1997. Selection by temperature of nitrate reducing bacteria from estuarine sediments: species composition and competition for nitrate. FEMS Microbiology Ecology 23, 11–22.

Paerl, H., Valdes, L., Pinckney, J., Piehler, M., Dyble, J., Moisander, P., 2003. Phytoplankton photopigments as indicators of estuarine and coastal eutrophication. Bioscience 53, 953–964.

Payne, W., 1981. Denitrification. Wiley.

Porubsky, W., Velasquez, L., Joye, S., 2008. Nutrient-replete benthic microalgae as a source of dissolved organic carbon to coastal waters. Estuaries and Coasts 31, 860–876.

Risgaard-Petersen, N., Nielsen, L., Rysgaard, S., Dalsgaard, T., Meyer, R., 2003. Application of the isotope pairing technique in sediments where anammox and denitrification coexist. Limnology and Oceanography. Methods 1, 63–73.

Risgaard-Petersen, N., Meyer, R., Schmid, M., Jetten, M., Enrich-Prast, A., Rysgaard, S., Revsbech, N., 2004. Anaerobic ammonium oxidation in an estuarine sediment. Aquatic Microbial Ecology 36, 293–304.

Rysgaard, S., Risgaard-Petersen, N., Nielsen, L., Revsbech, N., 1993. Nitrification and denitrification in lake and estuarine sediments measured by the ^{15}N dilution technique and isotope pairing. Applied and Environmental Microbiology 59, 2093–2098.

Seitzinger, S., 1994. Linkages between organic matter mineralization and denitrification in eight riparian wetlands. Biogeochemistry 25, 19–39.

Solorzano, L., 1969. Determination of ammonia in natural waters by the phenonl hypochlorite method. Limnology and Oceanography 14, 799–801.
Sørensen, J., Tiedje, J., Firestone, R., 1980. Inhibition by sulfide of nitric and nitrous oxide reduction by denitrifying *Pseudomonas flourescens*. Applied and Environmental Microbiology 39, 105–108.
Steward, J., Virnstein, R., Lasi, M., Morris, L., Miller, J., Hall, L., Tweedale, W., 2006. The impacts of the 2004 hurricanes on hydrology, water quality, and seagrass in the central Indian River Lagoon, Florida. Estuaries and Coasts 29 (6A), 954–965.
Strickland, J., Parsons, T., 1972. In: A Practical Handbook of Seawater Analysis, second ed. Bulletin of the Fisheries Research Board of Canada.
Sundbäck, K., Miles, A., Göransson, E., 2000. Nitrogen fluxes, denitrification and the role of microphytobenthos in microtidal shallow-water sediments: an annual study. Marine Ecology Progress Series 200, 59–76.
Thamdrup, B., Dalsgaard, T., 2002. Production of N_2 through anaerobic ammonium oxidation coupled to nitrate reduction in marine sediments. Applied and Environmental Microbiology 68, 1312–1328.
Thauer, R., Jungermann, K., Decker, K., 1977. Energy conservation in chemotrophic anaerobic bacteria. Micobiological Reviews 41, 100–180.
Tiedje, J., 1994. Denitrifiers. In: Weaver, R. (Ed.), Methods of Soil Analysis, Part 2. Soil Science Society of America, pp. 245–267.
Tiedje, J., Sexston, A., Myrold, D., Robinson, J., 1982. Denitrification: ecological niches, competition, and survival. Antonie van Leeuwenhoek Journal of Microbiology 48, 569–583.
Weston, N.B., Joye, S.B., 2005. Temperature driven accumulation of labile dissolved organic carbon in marine sediments. Proceedings of the National Academy of Sciences of the United States of America 102, 17036–17040.
Weston, N., Porubsky, W., Samarkin, V., MacAvoy, S., Erickson, M., Joye, S., 2006. Porewater stoichiometry of terminal metabolic products, sulfate, and dissolved organic carbon and nitrogen in estuarine intertidal creek bank sediments. Biogeochemistry 77, 375–408.
Wetz, M., Wheeler, P., 2007. Release of dissolved organic matter by coastal diatoms. Limnology and Oceanography 52, 798–807.
Windom, H., McKeller, H., Jr., Alexander, C., Jr., Craig, A., Abusam, A., Alford, M., 1998. Indicators of trends toward coastal eutrophication. Land use-coastal ecosystem study, State of Knowledge Report.
Zumft, W., 1992. The denitrifying prokaryotes. In: Balows, A., Trüper, H., Dworkin, M., Harder, W., Schleifer, K. (Eds.), The ProkayotesA Handbook on the Biology of Bacteria: Ecophysiology, Isolation, Identification, Applications, second ed, vol. 1. Springer-Verlag, pp. 554–582.